

Article

Water Hammer Characteristics and Component Fatigue Analysis of the Essential Service Water System in Nuclear Power Plants

Haonan Su ^{1,2}, Liyuan Sheng ^{2,3}, Shuai Zhao ^{1,2}, Cheng Lu ^{2,3}, Rongsheng Zhu ^{1,2}, Yiming Chen ^{1,2}
and Qiang Fu ^{1,2,*}

¹ National Research Center of Pumps, Jiangsu University, Zhenjiang 212013, China; 2212211021@stmail.ujs.edu.cn (H.S.)

² The Joint Lab of Intelligent O & M for NPP Pump, Zhenjiang 212013, China

³ China Nuclear Power Engineering Co., Ltd., Beijing 100048, China

* Correspondence: ujsfq@sina.com

Abstract: Due to the operation conditions and system characteristics of the essential service water system of nuclear power plants, water hammer pressure fluctuates in each transient process. In order to further analyze the characteristics of the water hammer and the harm this can cause to system equipment, this paper uses one-dimensional transient computing software to simulate the water hammer characteristics of the system under different operating conditions and at different water levels. The instantaneous pressure data of water hammer in the essential service water system were used as input conditions for fatigue analysis of components, and the fatigue damage of at-risk parts was calculated. The results show that the pressure fluctuation due to single pump outage is greater than that due to single pump start-up and the start-up of double pumps. The maximum pressure of the system under the design flood level is greater than that of other water levels, and the maximum pressure of the system under each working condition is 3.87 MPa. The most at-risk part of the system pressure fluctuation is the return valve, followed by the valve after a bend in a pipe and the tee pipe fitting. In the whole system, the joint of the main branch of a tee pipe experiences the greatest fatigue damage, and the theoretical fatigue life is 127.55 years.

Keywords: SEC; water hammer characteristics; check valve; fatigue analysis



Citation: Su, H.; Sheng, L.; Zhao, S.; Lu, C.; Zhu, R.; Chen, Y.; Fu, Q. Water Hammer Characteristics and Component Fatigue Analysis of the Essential Service Water System in Nuclear Power Plants. *Processes* **2023**, *11*, 3305. <https://doi.org/10.3390/pr11123305>

Academic Editors: Bivas Panigrahi and Blaž Likozar

Received: 21 September 2023

Revised: 11 November 2023

Accepted: 18 November 2023

Published: 27 November 2023



Copyright: © 2023 by the authors. Licensee MDPI, Basel, Switzerland. This article is an open access article distributed under the terms and conditions of the Creative Commons Attribution (CC BY) license (<https://creativecommons.org/licenses/by/4.0/>).

1. Introduction

In the operation of a pipeline system, due to the different working conditions, it is often necessary to switch the pipeline system and start or stop a pump and other operations. At the moment when the pump starts or stops, the flow rate changes rapidly, resulting in the instantaneous change in pressure, which is called water hammer [1]. The essential service water system (SEC) in a nuclear power plant functions as the ultimate heat sink of the plant, and as a nuclear safety system, the existence of the phenomenon of water hammer in the SEC is detrimental to the safe operation of the power plant. Figure 1 shows a common SEC system flowchart. As shown in the figure, upstream of the SEC is the seawater filtration system (CFI). During operation, the seawater is transported by the water pumps (01–44PO in the figure) through the check valves, pipeline, and shellfish traps (01–02FI), exchanging heat in the heat exchangers (001–004RF), taking away the heat brought by the equipment cooling water system (RRI), and finally flowing into the circulating water drainage channel from the overflow wells into the open sea [2].

Han et al. [3] used numerical calculation software to study water hammer characteristics in detail and obtained the optimal valve closing time under actual engineering conditions. Tian W et al. [4] conducted a transient analysis of the water hammer phenomenon of an SEC system and compared different protection schemes. Yao et al. [5] analyzed the influence of different valve openings on the operation of the pipeline network using MATLAB software and summarized the optimal degree of valve opening and the best

optimized operation scheme of the system. These studies mainly analyzed the effects of valve opening and closing time on water hammer, and the characteristics of water hammer were not specifically analyzed in the studies. As a famous thermal fluid system simulation and analysis software, Flowmaster is a great help in studying water hammer characteristics and has been adopted by world-renowned companies for its efficient computing efficiency, accurate solution ability, and convenient and fast modeling methods [6].

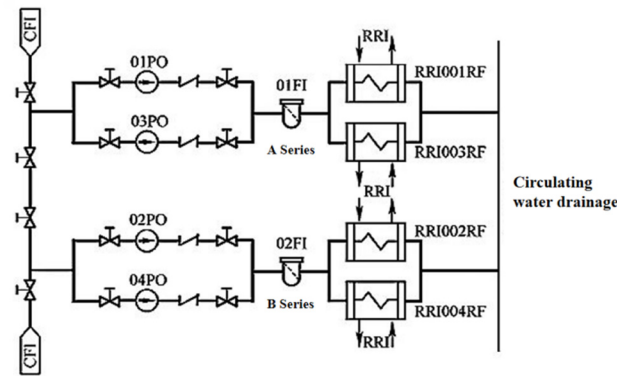


Figure 1. Flowchart of the SEC system.

Most researchers compared the maximum pressure of the pipeline at the time of water hammer to provide a basis for the selection of protective measures. Li et al. [7] studied the water hammer problem caused by the check valve when the pump was unexpectedly stopped. They found that the water hammer pressure is proportional to the flow rate, and an optimization method for reducing the water hammer pressure by closing the check valve was proposed. Zhao et al. [8] used a fluent dynamic mesh and UDF technology to simulate the steady flow characteristics of the fully opened valve and the transient flow characteristics during the closing process of the check valve. The results show that the pressure of water hammer decreases with the increase in closing time under certain closing modes. Other researchers have analyzed the hazards of transient pressure fluctuations to pipelines through fluid–structure interaction [9]. However, under the alternating action of pressure, the equipment may be damaged by fatigue. Therefore, focusing only on the maximum pressure does not completely guarantee the safety of the equipment, and equipment fatigue is also a factor that needs to be considered. Fatigue simulation is now widely used in the design and life prediction of mechanical equipment [10]. Ma Z et al. [11] conducted fatigue life simulation research on an automobile torsion beam, which proved that this method can quickly and effectively predict the fatigue life of parts and provide a basis for automobile design.

In summary, most researchers use one-dimensional simulation software to study the characteristics of the water hammer phenomenon of the pipeline system and use the calculated maximum pressure of the pipeline as the basis for the selection of water hammer protection measures, but there is only limited assessment of its hazard [5]. Therefore, in order to explore the fatigue damage of water hammer pressure fluctuations to equipment, in this research, numerical calculation of the water hammer in the SEC system of a power plant was carried out using Flowmaster to determine the parts of the system vulnerable to water hammer and their load time history. Then, fatigue simulation methods were used to quantitatively evaluate the hazards caused by water hammer to provide a theoretical basis for the subsequent water hammer protection measures of the SEC system and provide support for the long-term stable operation of nuclear power plants.

The rest of the paper proceeds as follows: Section 2 describes the materials and methods; Section 3 introduces the results and discussion; and Section 4 summarizes the conclusions.

2. Materials and Methods

2.1. Water Hammer Calculation Model for SEC Systems

Figure 2 depicts a schematic diagram of the pipeline direction of the SEC system. SEC systems are distinguished by their long pipelines and significant height differentials. The check valve and SEC pump are situated at a depth of 9 m below the seawater level, while the center elevation of the outlet pipe for the plate heat exchanger is approximately 16 m.

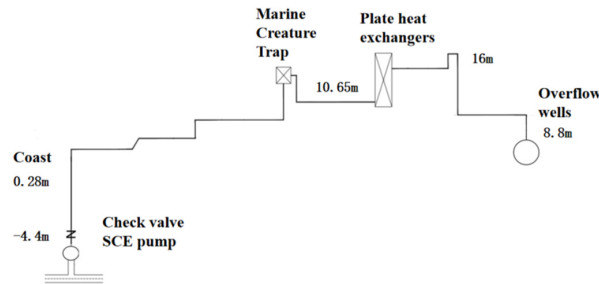


Figure 2. SEC system elevation map.

The specific data of the SEC system is shown in the following Table 1.

Table 1. Data of the SEC system.

Name	Parameter
Pumps	Flow rate 75 m ³ /h, head 25 m
Pipe length	395 m
Pipe vertical height difference	16 m
Pipe diameter	0.7 m
Check valve	HH44X-16

2.2. Fatigue Analysis Technology Route

To better assess the potential danger of water hammer under the first-stage butterfly check valve, in this section, we conducted a fatigue analysis to evaluate the possible damage caused by fluctuations.

The fatigue simulation involves several steps, including importing the geometry directly into ANSYS2020.2 Workbench, utilizing newly developed materials, and importing load data from the stress results of the structural calculation. The fatigue analysis module was then selected, and relevant parameters were set before calculating the fatigue life at each point of the structure.

The specific steps are illustrated in the following Figure 3.

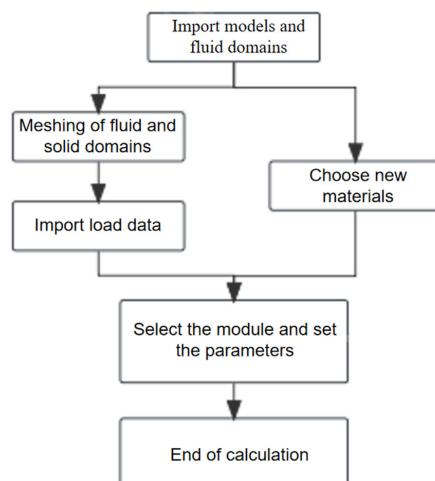


Figure 3. Fatigue simulation steps.

2.3. Steam Cavity Calculation Model and Boundary Condition Settings

2.3.1. Flowmaster Calculation Model

In this paper, Flowmaster2020.1 software was employed to simulate the water hammer of the SEC system. The principle involves treating the fluid pipeline as a series of fluid pipeline elements connected by nodes. The flow of each element is described by linearized continuity and momentum equations, simplifying the solution of the entire fluid system into a system of linear equations.

Continuity equation:

$$\bar{v} \frac{\partial h}{\partial x} + \frac{\partial h}{\partial t} \bar{v} \sin \alpha + \frac{\alpha^2}{g} \frac{\partial v}{\partial x} = 0 \quad (1)$$

Momentum equation:

$$g \frac{\partial h}{\partial x} + \bar{v} \frac{\partial \bar{v}}{\partial x} + \frac{\partial \bar{v}}{\partial t} + \frac{f \bar{v} |\bar{v}|}{2D} = 0 \quad (2)$$

where h is the frictional head; v is the average velocity of the fluid in the cross-section; g is the gravity acceleration; f is the friction factor; α is the angle between the center line and the horizontal line of the pipeline; D is the diameter of the pipe; a is the wave speed.

In the simulation, the overall linear equation system of the entire fluid network was solved to obtain the flow rate and head parameters of each component at steady state. Subsequently, the eigenline method was applied to calculate the transient process. A fluid network consists of a series of piping elements, each primarily modeled on the pressure–flow relationship [4].

Given that the inlet and outlet of the valve are connected to the inlet and outlet pipes through flanges and the pipes are fixed by the pipe piers, it is assumed that the inlet and outlet of the valve and the pipe fittings do not displace, and fixed constraints are imposed.

2.3.2. CFD Calculation Model

The k-Epsilon turbulence model [12,13] is used for the calculation domain and the specific equation is as follows.

$$\rho \frac{dk}{dt} = \frac{\partial}{\partial x_i} \left[\left(\mu + \frac{\mu_t}{\sigma_k} \right) \frac{\partial k}{\partial x_i} \right] + G_k + G_b - \rho \epsilon - Y_M \quad (3)$$

$$\rho \frac{d\epsilon}{dt} = \frac{\partial}{\partial x_i} \left[\left(\mu + \frac{\mu_t}{\sigma_\epsilon} \right) \frac{\partial \epsilon}{\partial x_i} \right] + G_{1\epsilon} \frac{\epsilon}{k} (G_k + G_{3\epsilon} G_b) - C_{2\epsilon} \rho \frac{\epsilon^2}{k} \quad (4)$$

$$G_k = \rho \frac{\epsilon^2}{k} C_\mu \left(\frac{\partial \mu_i}{\partial x_j} + \frac{\partial \mu_j}{\partial x_i} \right) \quad (5)$$

where $G_{1\epsilon}$, $G_{2\epsilon}$, and G_μ are empirical constants of 1.44, 1.92, and 0.09, respectively.

The calculation model of the steam cavity [14,15] is shown below.

$$\begin{aligned} & \frac{\partial}{\partial t} \left(\sum_{k=1}^2 \frac{1}{2} \overline{\rho_k v_{kx}^2} \right) + \frac{\partial}{\partial x_\beta} \left(\sum_{k=1}^2 \frac{1}{2} \overline{\rho_k v_{kx}^2 v_{k\beta}} \right) \\ = & - \frac{\partial}{\partial x_\alpha} \left(\sum_{k=1}^2 \overline{\rho_k P'_{k\alpha} v'_{k\alpha}} \right) - \frac{\partial}{\partial x_\beta} \left(\sum_{k=1}^2 \frac{1}{2} \overline{\rho_k \rho_k v'_{k\alpha} v'_{k\beta}} \right) + \frac{\partial}{\partial x_\beta} \left(\sum_{k=1}^2 \overline{\rho_k \tau'_{k\alpha\beta} v'_{k\alpha}} \right) - \sum_{k=1}^2 \left(\overline{\rho_k \tau'_{k\alpha\beta} \frac{\partial v'_{k\alpha}}{\partial x_\beta}} \right) \\ & - \sum_{k=1}^2 \overline{\rho_k \rho_k v'_{k\alpha} v'_{k\beta} \frac{\partial v'_{k\alpha}}{\partial x_\beta}} + \sum_{k=1}^2 \overline{\rho_k \rho_k F'_{k\alpha} v'_{k\alpha}} - \sum_{k=1}^2 \overline{(P'_{ki} v'_{k\alpha i} n_{ki\alpha} a_i)} + \sum_{k=1}^2 \overline{(\tau'_{k\alpha\beta i} v'_{k\alpha i} n_{ki\beta} a_i)} \end{aligned} \quad (6)$$

Here, ρ_k , v_k , τ_k , F_k , U_k , q_k and Q_k are the density, velocity (vector), pressure, stress tensor, external force (vector), internal energy, heat flux (vector) and internal heat generation rate of phase k ; v_i is the velocity vector of the interface and the subscript k_i denotes the value of phase k at the interface; and n_{ki} is the normal outward unit vector of phase k at the interface [14].

Based on the calculation results of water hammer characteristics, the fatigue simulation condition compiled the load spectrum of each component according to the pressure fluctuation time history diagram obtained in the second section. As a boundary condition, it was imported and calculated by loading historical data. The position of the pressure load was on the inner surface of the pipe fittings and the wall behind the valve plate of the check valve equipment.

2.4. Model Building and Meshing

The essential service water system of each unit contains two series and four pumps. Under normal circumstances, only one pump of one series needs to be operated, while the other series is out of operation. Taking one of the series as the research object (as shown in Figure 2), this paper established the water hammer calculation and analysis model as in the following Figure 4.

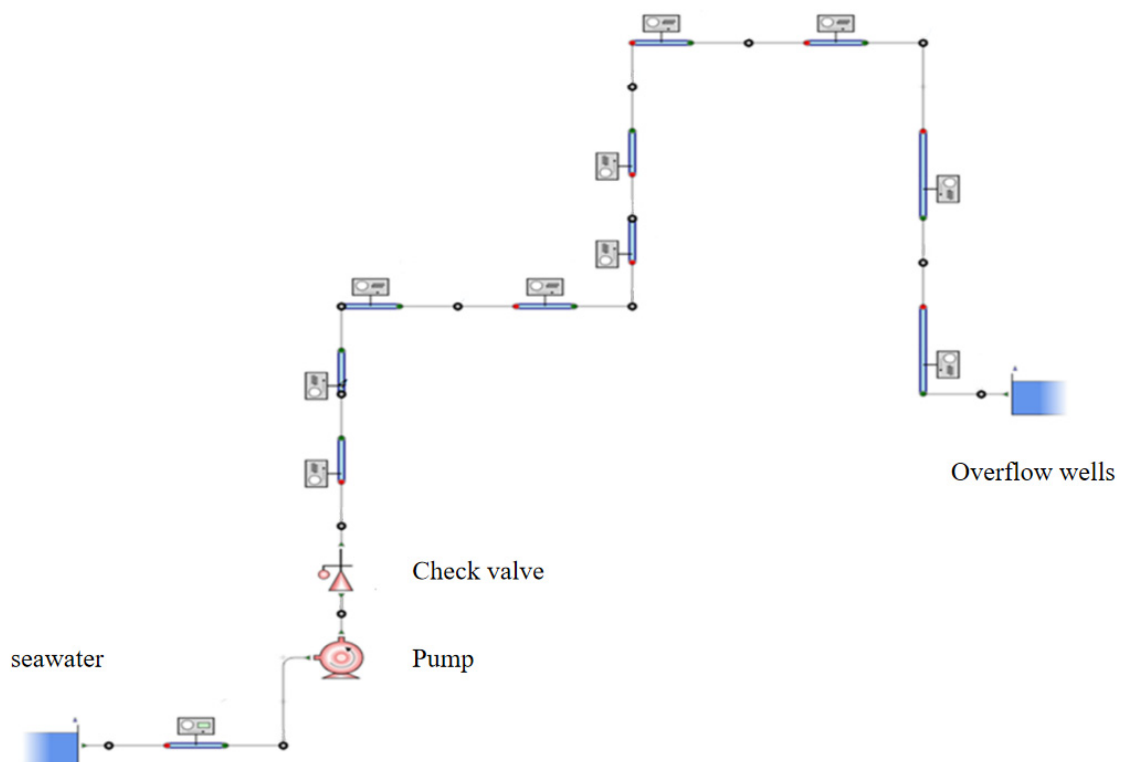


Figure 4. Schematic diagram of the water hammer characterization model.

In the section on CFD calculation, it is worth noting that the long pipeline, numerous components, and intricate structure of heat exchangers make it challenging to model the entire system comprehensively. As a result, this study primarily focused on calculating and analyzing the local pipe fittings and equipment of the system, such as elbows, tees, and butterfly check valves. The model is shown in Figure 5.

The models were constructed based on the outline and assembly drawings supplied by the power plant, with the nominal diameter of the valve and pipe fittings set at 700 mm. During the three-dimensional modeling of the check valve, the valve body and the valve plate were identified as the most important components and were therefore retained for subsequent calculations, as depicted in Figure 6. However, certain parts that have minimal impact on the calculation results were found to increase the mesh complexity and count. As a result, non-critical components, such as the valve stem and handle, were removed from the model.

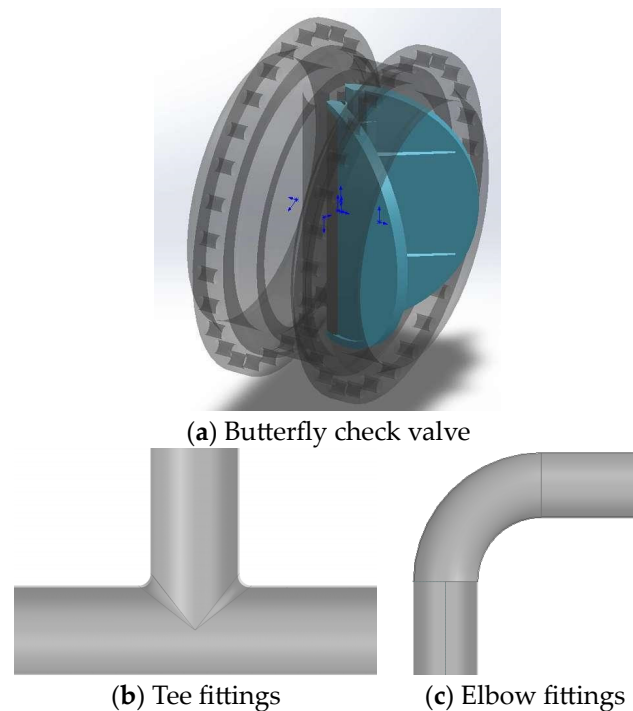


Figure 5. Three-dimensional models.

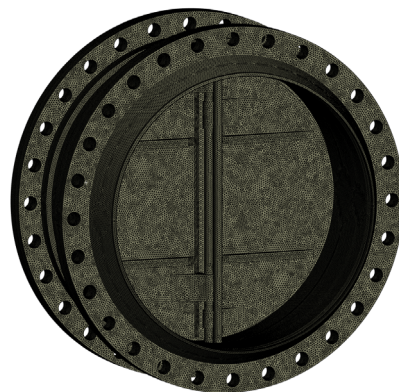


Figure 6. Grid of check valves.

Solid region meshing was carried out using ANSYS Workbench, offering a range of meshing methods to cater to diverse model requirements, including auto-partitioning, tetrahedral meshing, hexahedral meshing, sweeping, and multi-zone methods. Given the complex structure of the check valve, tetrahedral meshing was employed to divide it. The grid quality was assured to be above 0.4 through module evaluation, and the grid independence test was conducted by calculating the equivalent force at maximum pressure. Ultimately, the number of grid cells for the butterfly check valve amounts to 2,646,789, as depicted in Figure 6.

2.5. Material Fatigue Properties

Based on the given information, the primary material utilized for the butterfly check valve is UNS S32750, while the pipeline material for the vital plant water system is typically carbon steel P265GH. The material properties of the latter are comparable to the domestic Q245R, and the S-N curve was obtained through fitting based on the material properties. The material properties of the valve body and pipe fittings are shown in Table 2.

Table 2. Material property table of valve body and pipe fittings.

Material	Yield Strength MPa	Tensile Strength MPa	Elastic Modulus GPa
SAF2507	572	950	175
P265GH	265	410	204

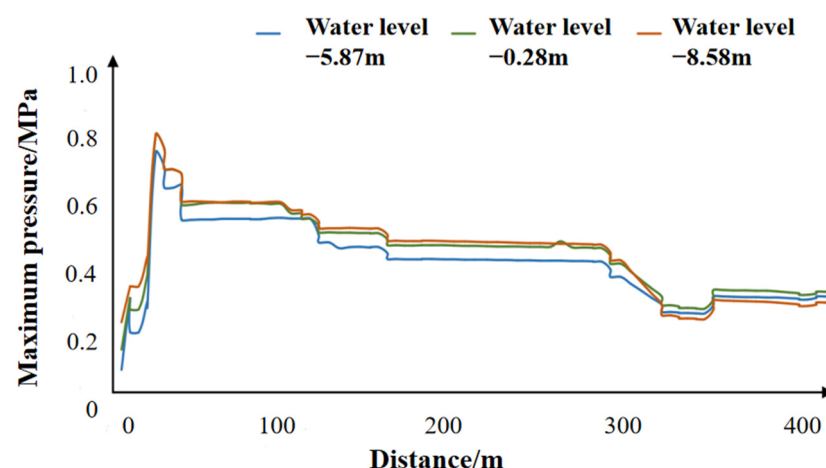
3. Results and Discussion

3.1. SEC System Water Hammer Characterization

Using the water hammer analysis model described above, we conducted an analysis of the water hammer characteristics of the SEC system. The check valve in the SEC system is a butterfly check valve, designed to close rapidly after the pump is stopped. According to this model, the theoretical closing time of the butterfly check valve is set at 0.1 seconds.

This study encompassed three different water levels: the design minimum water level (−5.87 m), the average water level (0.28 m), and the design maximum water level (8.58 m). Each water level included scenarios such as single pump operation stop, single pump operation start, stop operation of one pump during parallel operation of double pumps, and starting the pump when another single pump operates.

Figures 7 and 8 depict the calculated results of the maximum pressure and maximum steam cavity within the system pipeline under the conditions of single pump operation and single pump shutdown at the design minimum water level (−5.87 m), average water level (0.28 m), and design maximum water level (8.58 m). It is evident that the maximum pressures within the pipeline are 0.712, 0.764, and 0.765 MPa, with the check valve and its rear being identified as the primary sites for maximum pressure generation. This phenomenon occurs because when the pump stops, the downstream water flow loses momentum, leading to a reverse flow towards lower water levels. Simultaneously, the closed check valve rapidly blocks and accumulates the flowing liquid, resulting in a pressure surge at the check valve location. When considering the maximum cavity calculation results, the formation of a decompression wave within the system leads to a pressure reflection, causing the pressure to reach the saturated vapor pressure at a specific position. Consequently, a cavitation is formed, particularly after the heat exchanger, due to its elevated position and maximum negative pressure, resulting in the largest steam cavity, measuring up to 600 mm in length. The presence of a steam cavity further exacerbates water hammer fluctuations.

**Figure 7.** Double pump operation, single pump stop operation line maximum pressure diagram.

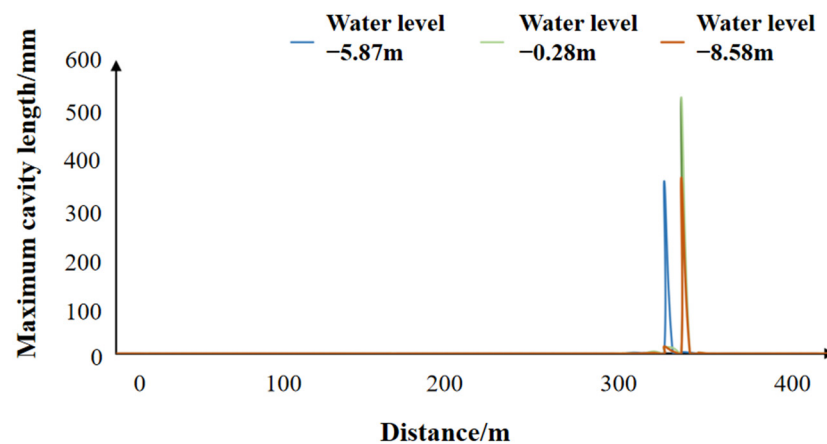


Figure 8. Diagram of the maximum steam cavity length of the single pump decommissioning line for double pump operation.

Figure 9 displays the pressure fluctuation of the check valve and tee part under three different water levels with time. At the moment when the pump stops, the flow pressure decreases, and after the pressure is reduced to the minimum, there is a certain recovery. This is due to the liquid column being farther forward due to inertia and then rebounding due to low pressure. For the check valve, the pressure begins to fluctuate slightly after recovery, and then the first water hammer boost occurs due to the recoil of the counterflow liquid. When the liquid column flows back again, the second water hammer boost occurs. After several fluctuations, the energy of the fluid is gradually converted, and the pressure tends to stabilize. Compared with the check valve and other parts, the pressure rise at the check valve is slightly earlier, and the maximum pressure is much greater than in other positions, which is consistent with the analysis of this process.

Further, other working conditions were calculated, and the results were obtained as the following Table 3.

Table 3. Summary of maximum pressure in SEC system pipelines.

Mode	Working Conditions	Description of the Operating Condition	Maximum Pressure (MPa)
The water pump stops	1	At low tide levels, one pump stop operation when single pump is running	3.42
	2	At low tide levels, one pump is out of operation when two pumps are running in parallel.	0.712
	3	At average tide levels, one pump stop operation when single pump is running	3.53
	4	At average tide levels, one pump is out of operation when two pumps are running in parallel.	0.764
	5	At high tide levels, one pump stop operation when single pump is running	3.87
	6	At high tide levels, one pump is out of operation when two pumps are running in parallel.	0.765
The water pump starts	7	At low tide levels, single pump is running	0.72
	8	At low tide levels, starting another pump when single pump is running	0.61
	9	At average tide levels, single pump is running	0.74
	10	At average low tide levels, start another pump when the single pump is running	0.63
	11	At high tide levels, single pump is running	0.84
	12	At high low tide levels, start another pump when the single pump is running	0.724

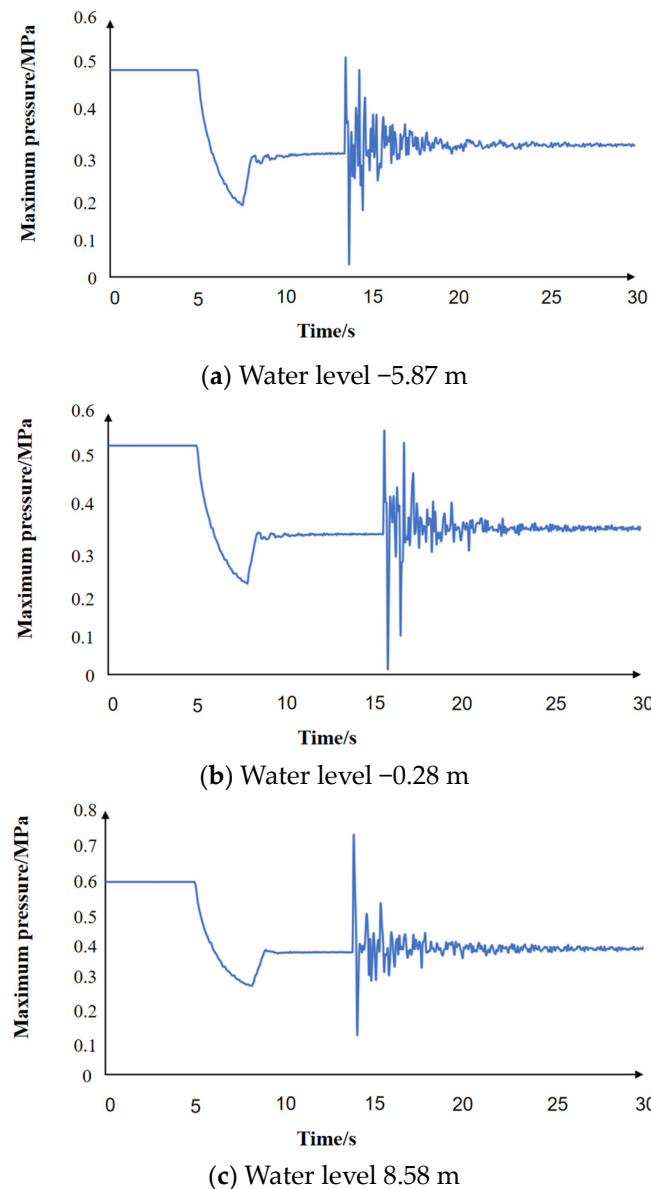


Figure 9. Pressure fluctuations after different water level check valves.

The calculation results reveal that under different seawater tide levels, the system pressure at high tide exceeds other water levels. In most working conditions, the maximum system pressure barely reached 1 MPa. However, when a single pump was stopped, the pressure fluctuation caused by water hammer increased significantly, with the maximum system pressure reaching 3.87 MPa, more than five times that of other working conditions.

3.2. Fatigue Simulation Calculation Results

Through the relentless efforts of scholars, fatigue research has evolved into a comprehensive system that can be applied to engineering practice and has become a leading research area, largely through the utilization of finite element simulation analysis software. Fatigue simulation calculations enable the determination of the minimum number of cycles in different parts of the simulation model and the visualization of the fatigue life distribution on the object's surface using a cloud map on the model [16–19]. Computer-aided engineering (CAE) is a virtual simulation that accurately responds to load stress and can provide precise simulations of fatigue endurance life [20–24]. Chiriță P. A. et al. [19] analyzed the effects of variable pressure on the life of hydraulic gear pumps using modern

numerical simulation tools (CAE and CAD). Their study presents the results of static and dynamic analysis (fatigue) as well as experimentation, validating these simulations.

Compared to traditional fatigue analysis methods, CAE fatigue simulation technology can display the fatigue life distribution of the object's surface in three dimensions and multiple angles, providing a more intuitive understanding of the overall fatigue life distribution of the object under study. Therefore, the CAE fatigue analysis method is specifically used to demonstrate the fatigue life distribution of valves. In this study, since the wave load is caused by water hammer, the minimum number of cycles obtained from the calculation results represents the number of water hammer fluctuations that different positions of the equipment can withstand.

3.2.1. Pipe Fittings

Based on the 1, 3, and 5 working conditions where fatigue damage is most obvious, the fatigue calculation results of the following components were analyzed. The number of fatigue cycles of tee pipe fittings and bending under different working conditions are shown in Figures 10 and 11.

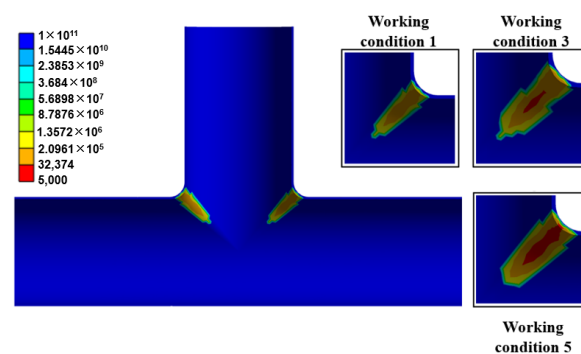


Figure 10. The number of fatigue cycles of tee pipe fittings under different working conditions.

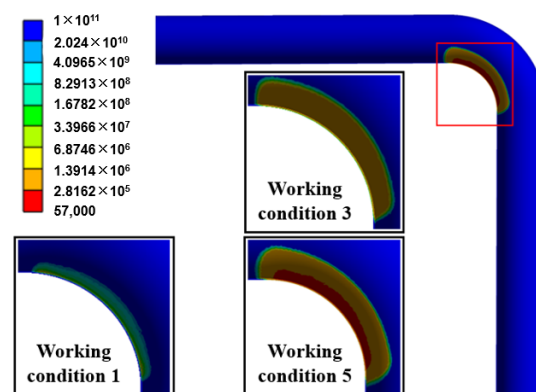


Figure 11. The number of fatigue cycles of bending under different working conditions.

After analyzing the fatigue calculation results under a single working condition, it was found that for tee pipe fittings, the location with greater damage is usually at the connection between the main pipe and the branch pipe due to stress concentration. For pipe bends, the location with greater damage is typically on the inside of the elbow, also due to stress concentration. Comparing different working conditions, the most dangerous working conditions for both parts are the operation of the single pump under the one-stage check valve design reference flood level. The minimum number of cycles for the tee pipe fittings is 6304 times, while for the bending pipe, it is 57,552 times. In comparison, the elbow part has a longer fatigue life than the tee part.

3.2.2. Check Valve

The number of fatigue cycles of the check valve under different working conditions is shown in Figure 12. For butterfly check valves, the primary source of fatigue damage is the root of the valve plate shaft. This is because under alternating loads, the entire valve plate is subjected to pressure, and the valve plate is fixed by the rotating shaft, leading to stress concentration at the fixed position of the shaft and the valve body. The calculation results of different working conditions indicate significant fluctuations in working conditions 1, 3, and 5, resulting in more fatigue damage under these conditions. However, under other working conditions, the overall wall thickness of the check valve is thicker, and the material properties are better. As a result, even if the pressure fluctuation amplitude at the check valve is greater than that of other parts, from a fatigue perspective, the degree of pressure fluctuation does not cause a significant impact.

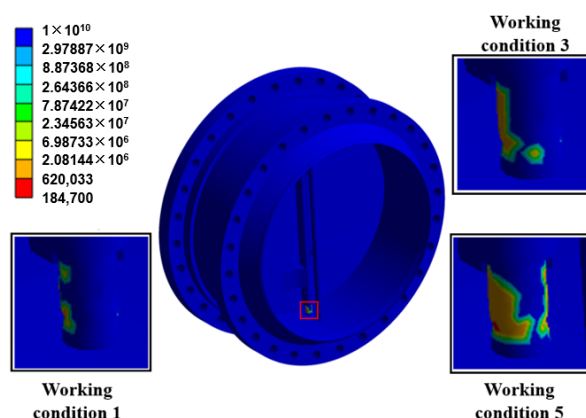


Figure 12. The number of fatigue cycles of the check valve under different working conditions.

Table 4 is the summary of the minimum fatigue cycles. The calculation results reveal that the most damaging working condition for all components is single pump operation shutdown. In contrast, the pressure fluctuation resulting from the starting condition and the double pump operating condition is minimal, leading to weaker fatigue damage. Despite the more severe pressure fluctuations at the check valve, the tee pipe experiences more significant stress concentration, resulting in a smaller minimum number of fatigue cycles and a shorter fatigue life. This suggests that the tee pipe is more susceptible to fatigue damage despite the severe pressure fluctuations at the check valve, owing to the superior material performance of the check valve.

Table 4. Summary of minimum fatigue cycles.

Working Conditions	Tee	Elbows	One-Stage Check Valve
1	33,048	260,721	516,124
2	1×10^{11}	1×10^{11}	1×10^{10}
3	13,717	120,084	381,518
4	1×10^{11}	1×10^{11}	1×10^{10}
5	6304	57,552	184,786
6–12	1×10^{11}	1×10^{11}	1×10^{10}

3.3. Estimated Lifetime Calculation

Based on the aforementioned research, the minimum fatigue cycle times for different working conditions of the three equipment were calculated, representing the number of times the equipment can withstand corresponding water hammer working conditions. To further assess the fatigue-related calculation results in annual measurement cycles, the following calculation rules were adopted:

For different working conditions, it was assumed that each water level and the probability of single pump and double pump operation conditions were the same. Each unit consisted of two series, each operating for an average of 50% of the time per year. The time of starting and stopping under each working condition was one-twelfth of the year, and the pressure fluctuation of each working condition occurred 30 times a year according to the daily start and stop. Assuming the total life cycle is 1, the proportion of damage caused by fluctuations under a certain working condition every year was calculated using the following formula:

$$S_x = \frac{30}{N_x} \quad (7)$$

Among them, S_x is the fatigue damage caused by water hammer under the working condition x every year;

N_x is the minimum number of fluctuations in case x , which is found in Table 4 of the calculation results.

The results are presented below, with the figures in Table 5 representing the proportion of damage in the total life.

Table 5. Annual fatigue damage table for different working conditions.

Working Conditions	Tee	Elbows	One-Stage Check Valve
1	9.08×10^{-4}	1.15×10^{-5}	5.81×10^{-5}
2	3×10^{-10}	3×10^{-10}	3×10^{-9}
3	2.18×10^{-3}	2.49×10^{-5}	7.86×10^{-5}
4	3×10^{-10}	3×10^{-10}	3×10^{-9}
5	4.76×10^{-3}	5.21×10^{-4}	1.62×10^{-4}
6–12	3×10^{-10}	3×10^{-10}	3×10^{-9}
total	7.84×10^{-3}	5.57×10^{-4}	2.98×10^{-4}

Based on the calculations, the largest damage is 7.85×10^{-3} , and the maximum number of years it can withstand is its reciprocal, indicating an estimated lifespan of 127.55 years.

In summary, the life calculation results demonstrate that the pressure fluctuation phenomenon of pump shutdown transient has a certain impact on the safe operation of the system. Although the impact is still within a long time range, it can lead to greater harm due to equipment corrosion, aging, defects, defects in the metal itself, and even the impact of water hammer cavitation collapse. Therefore, even though numerical simulation methods provide conservative results and the outcomes are still within a reliable time range, pressure fluctuations can still cause some damage.

4. Conclusions

The operation conditions and system characteristics of the essential service water system in nuclear power plants result in water hammer pressure fluctuations during each transient process. The objective of this study was to analyze the water hammer characteristics and the potential harm to the system equipment in order to provide a theoretical basis for subsequent water hammer protection measures of the SEC system and support the long-term stable operation of nuclear power plants.

Traditionally, most researchers have compared the maximum pressure of the pipes in the event of water hammer to inform the selection of protective measures. However, under the alternating action of pressure, equipment can be damaged due to fatigue. Therefore, focusing solely on the maximum pressure does not fully guarantee the safety of the equipment. In an effort to explore the fatigue damage caused by water hammer pressure fluctuations to equipment, this study innovatively combined Flowmaster software and fatigue simulation to quantitatively evaluate the hazards caused by water hammer. This approach aims to provide a more comprehensive understanding of the potential damage and offer a theoretical basis for the development of effective water hammer protection

measures for the SEC system, ultimately supporting the long-term stable operation of nuclear power plants.

Among the 12 water hammer conditions of the SEC system, the water hammer hazard degree fluctuated the most during single pump operation stop. The designed flood levels pose the most significant risk, with the check valve and its subsequent tee and elbow identified as the most vulnerable parts. Corresponding protection measures can be implemented through operational control.

Under the pressure load from different water hammer conditions, the most vulnerable part of the tee pipe is the connection position between the main pipe and the branch pipe. Similarly, the inside of the bending part is the dangerous position of the bend, and the root of the valve plate shaft is the most vulnerable part of the check valve. Generally, the tee is the most susceptible position. Targeted reinforcement can be carried out in the power plant's equipment arrangement to address these vulnerabilities.

The fatigue simulation analysis of the water hammer characteristics of the SEC system and local equipment fatigue damage provides valuable insights for the quantitative evaluation of water hammer hazards. It also offers a theoretical basis for subsequent water hammer protection measures and supports the long-term stable operation of nuclear power plants.

While this study provides valuable insights into the hazards of pressure fluctuations to system equipment from a fatigue perspective, it is important to acknowledge that complex studies related to nuclear power and fluid systems cannot be achieved overnight. As such, the following research perspectives are worth further exploration: further study of the hazards of transient pressure fluctuations and in-depth research on the fatigue test of pipelines and equipment to address the inevitable errors in numerical simulation work and enhance calculation accuracy.

Author Contributions: Conceptualization, Q.F.; Methodology, R.Z.; writing—original draft, H.S.; software, S.Z.; validation, Y.C.; investigation, C.L.; funding acquisition, L.S. All authors have read and agreed to the published version of the manuscript.

Funding: Key Project of the Joint Fund of the National Natural Science Foundation of China (U20A20292).

Data Availability Statement: All data and models generated or used during the study appear in the submitted article.

Conflicts of Interest: The authors declare no conflict of interest.

References

1. Cao, Y.; Dou, Y.; Huang, Y.; Cheng, J. Study on Vibration Characteristics of Fracturing Piping in Pump-Starting and Pump-Stopping Water Hammer. *J. Fail. Anal. Prev.* **2019**, *19*, 1093–1104. [[CrossRef](#)]
2. Durbin, P.A. Separated flow computations with the k-epsilon-v-squared model. *AIAA J.* **1995**, *33*, 659–664. [[CrossRef](#)]
3. Han, Y.; Shi, W.; Xu, H.; Wang, J.; Zhou, L. Effects of closing times and laws on water hammer in a ball valve pipeline. *Water* **2022**, *14*, 1497. [[CrossRef](#)]
4. Tian, W.; Su, G.; Wang, G.; Qiu, S.; Xiao, Z. Numerical simulation and optimization on valve-induced water hammer characteristics for parallel pump feedwater system. *Ann. Nucl. Energy* **2008**, *35*, 2280–2287. [[CrossRef](#)]
5. Yao, E.; Kember, G.; Hansen, D. Analysis of water hammer attenuation in applications with varying valve closure times. *J. Eng. Mech.* **2015**, *141*, 04014107. [[CrossRef](#)]
6. Liu, B.; Wang, H.; Huang, Y.; Tang, G.; Ye, C. Research of Water Hammer of Air Conditioning Chilled Water System Based on Flowmaster. In Proceedings of the 2016 2nd International Conference on Advances in Mechanical Engineering and Industrial Informatics (AMEII 2016), Hangzhou, China, 9–10 April 2016; Atlantis Press: Paris, France, 2016; pp. 590–593.
7. Yang, G.; Li, M.; Bai, G.; Xu, M. Theoretical Analysis and Simulation of Buffer Cylinder for Anti-Water Hammering. In Proceedings of the 2018 International Conference on Mechanical, Electronic, Control and Automation Engineering (MECAE 2018), Qingdao, China, 30–31 March 2018.
8. Heng, Z.; Zhou, Z.; Peng, W. Research on Water Hammer Phenomenon during Stop Valve Closing Process Based on CFD. In Proceedings of the Big Data and Artificial Intelligence, Beijing, China, 22–24 June 2018; pp. 139–145.
9. Cherian, R.M.; Sajikumar, N.; Sumam, K.S. Influence of fluid–structure interaction on pressure fluctuations in transient flow. *J. Pipeline Syst. Eng. Pract.* **2021**, *12*, 04021002. [[CrossRef](#)]

10. Stromeyer, C.E. The determination of fatigue limits under alternating stress conditions. *Proc. R. Soc. London. Ser. A Contain. Pap. A Math. Phys. Character* **1914**, *90*, 411–425.
11. Ma, Z.; Huang, Y.; Ren, Z.; Zhang, Y.; Zhang, X. Analysis of key technology in fatigue simulation experiment of torsion beam. In Proceedings of the International Conference on Sensors and Instruments (ICSI 2021), Qingdao, China, 28–30 May 2021; SPIE: Philadelphia, PA, USA, 2021; Volume 11887, pp. 327–332.
12. Launder, B.E.; Spalding, D.B. *Mathematical Models of Turbulence*; Academic Press: London, UK, 1972; pp. 90–110.
13. Yakhot, V.; Orzag, S.A. Renormalization group analysis of turbulence. *I. Basic theory. J. Sci. Comput.* **1986**, *1*, 3–11. [[CrossRef](#)]
14. Kataoka, I.; Serizawa, A. Basic equations of turbulence in gas-liquid two-phase flow. *Int. J. Multiph. Flow* **1989**, *15*, 843–855. [[CrossRef](#)]
15. Gotawala, D.R.; Gates, I.D. Steam fingering at the edge of a steam chamber in a heavy oil reservoir. *Can. J. Chem. Eng.* **2008**, *86*, 1011–1022. [[CrossRef](#)]
16. Riduwan, P.; Andoko, A.; Suprayitno, S. Camshaft failure simulation with static structural approach. *J. Mech. Eng. Sci. Technol.* **2021**, *5*, 47–61.
17. Teng, T.Z.; Cai, Q.Z.; Jiang, H.H. Research on fatigue performance of offshore wind turbine blade with basalt fiber bionic plate. *Structures* **2023**, *47*, 466–481.
18. Xiao, X.; Zhang, H.; Li, Z.; Chen, F. Effect of temperature on the fatigue life assessment of suspension bridge steel deck welds under dynamic vehicle loading. *Math. Probl. Eng.* **2022**, *2022*, 1–14. [[CrossRef](#)]
19. Yang, H.X.; Li, X.P.; Xu, J.C.; Guo, Y.; Li, B. Modeling and fatigue characteristic analysis of the gear flexspline of a harmonic reducer. *Mathematics* **2022**, *10*, 868. [[CrossRef](#)]
20. Chiriță, P.A.; Popescu, T.C.; Marinescu, A.D.; Teodoru, C.; Crețu, C. Influence and Effects of Pressure Variation on the Life Span of External Gear Pumps. *Hidraulica* **2019**, *1*, 88–97.
21. Fu, M.W.; Yong, M.S.; Muramatsu, T. Die fatigue life design and assessment via CAE simulation. *Int. J. Adv. Manuf. Technol.* **2008**, *35*, 843–851. [[CrossRef](#)]
22. Tong, K.K.; Yong, M.S.; Fu, M.W.; Muramatsu, T.; Goh, C.S.; Zhang, S.X. CAE enabled methodology for die fatigue life analysis and improvement. *Int. J. Prod. Res.* **2005**, *43*, 131–146. [[CrossRef](#)]
23. Yim, H.J.; Lee, S.B. An integrated CAE system for dynamic stress and fatigue life prediction of mechanical systems. *KSME J.* **1996**, *10*, 158–168. [[CrossRef](#)]
24. Koh, S.K.; Lee, S.I.; Chung, S.H.; Lee, K.Y. Fatigue design of an autofrettaged thick-walled pressure vessel using CAE techniques. *Int. J. Press. Vessel. Pip.* **1997**, *74*, 19–32. [[CrossRef](#)]

Disclaimer/Publisher’s Note: The statements, opinions and data contained in all publications are solely those of the individual author(s) and contributor(s) and not of MDPI and/or the editor(s). MDPI and/or the editor(s) disclaim responsibility for any injury to people or property resulting from any ideas, methods, instructions or products referred to in the content.